JOURNAL OF MATERIALS SCIENCE 26 (1990) 6190–6196

Mechanical alloying of the Ti–Al system

W. GUO, S. MARTELLI, N. BURGIO, M. MAGINI, F. PADELLA, E. PARADISO
Amorphous Materials Project, E.N.E.A.-Casaccia C.P. 2400, I-00100 Roma, Italy
I. SOLETTA
Chemistry Department, University of Sassari, Via Vienna 2, I-07100 Sassari, Italy

Ti–Al alloys have been prepared by mechanical alloying (MA) of pure titanium and aluminium powders for four compositions: $Ti_{80}Al_{20}$, $Ti_{75}Al_{25}$, $Ti_{50}Al_{50}$, and $Ti_{40}Al_{60}$. The $50 < Ti(at\%) < 80$ compositions could be fully amorphized with a milling time strongly dependent on the starting chemical composition. For the $Ti_{40}Al_{60}$ composition, only partial amorphization was observed. The investigation on the early stage of MA shows that the different systems amorphized through two different paths. On the titanium rich side (Ti = 75,80 at%), the MA first leads to the formation of an h.c.p. αTi(Al) solid solution with an aluminium content of 14–16%, which subsequently collapses into the amorphous state. For the aluminium rich side (Al = 50,60 at%), MA sooner promotes the nucleations of disordered forms of Ti_3Al and TiAl intermetallic compounds, respectively. The inhibition of the ordering transition of the observed intermetallic phases is ascribed to the low temperature at which the SSR takes place. The complete ($Ti_{50}Al_{50}$) or partial ($Ti_{40}Al_{60}$) amorphization of the powder is then attained through a destabilization of the disordered Ti_3Al and TiAl phases. The present results confirm the existence of a metastable f.c.c. phase as final alloying stage for the $Ti_{75}Al_{25}$ and $Ti_{40}Al_{60}$ compositions.

1. Introduction

There is a considerable interest in titanium aluminides because of their attractive properties at elevated service temperatures. But, on the other hand, their low ductility and poor formability restrict considerably their industrial application [1]. A great effort has been devoted in recent years to improve the properties of Ti–Al alloys by means of chemistry modification and microstructure control. For instance, mechanical alloying (MA) is nowadays commercially exploited to produce aluminium titanium alloys with additional dispersoids. MA has also been revealed as a valuable tool to produce amorphous powders starting from pure elemental powders at a relatively low cost. Over the last few years, a number of works have been dedicated to the investigation of the low temperature solid state reaction (SSR) which can be originated in binary systems by imparting a severe plastic deformation, as in the case of high energy ball milling or cold rolling (see [2] for a comprehensive review). This kind of SSR may either lead to the formation of metastable phases, mostly amorphous, or lead to the formation of equilibrium intermetallic compounds. Besides the technological applications, the Ti–Al system is of great interest from a basic point of view because it cannot be amorphized by melt spinning or other rapid quenching techniques. In addition, since the Ti–Al system is quite similar to that of Zr–Al [4], it is well-suited for further investigation of the principle underlying the crystal to glass phase transition.

The feasibility of amorphizing Ti–Al by MA has already been tested [5–7], and a thermodynamic model predicting the formation, at room temperature, of amorphous alloys for compositions $25 < Ti\ (at\%) < 80$, has been proposed [6]. However, the literature results show some disagreements as far as the compositional range of amorphization is concerned. They also report the formation of a metastable f.c.c. phase, for the $Ti_{75}Al_{25}$ composition, when MA is performed beyond the complete amorphization.

In this context, we found it useful to obtain further information on the Ti–Al system submitted to the mechanical alloying process. Keeping in mind possible technological applications, the Ti–Al starting mixtures have been selected to approach the chemical compositions of the alloys based on titanium aluminides such as α_2-alloys and γ-alloys. Particular attention has been given to the early stage of MA since a knowledge about the onset of SSR is essential for understanding the reaction path followed by the system during ball milling.

2. Experimental procedure

Pure Ti (99.0%, 325 mesh) and Al (99.3%) (Alfa products) were used as starting powders. Mechanical alloying was carried out in a Frisch Pulverisette planetary mill with hardened steel vials and balls. The ball-to-powder weight ratio was approximately 10 : 1. In order to minimize oxygen contamination the vials were sealed under pure argon. The four different compositions, Ti_xAl_{1-x} (x = 40, 50, 75, 80 at%), were milled in exactly the same conditions and at the same time in the four places ball mill. To avoid an excessive

0022–2461/91 $03.00 + .12

warming up during milling, the vials were cooled by an air flow and a milling period of 30 min was alternated with an equal rest time. Small quantities of powder were withdrawn from the vials periodically for X-ray monitoring of the process.

X-ray diffraction patterns were recorded by automatic Seifert Pad IV and GSD diffractometers, using MoK_α (K_α = 0.07107 nm) radiation. To gain further information on the intermediate state of alloying, X-ray diffraction patterns of some representative samples were also recorded with a high resolution diffractometer (Italstructures X-red) equipped with a 120° curved multichannel position sensitive detector, a Johanson's monochromator on the incident beam (parafocussing geometry) and a Co target ($K_{\alpha 1}$ = 0.1789 nm). The recorded diffraction patterns were corrected for the background arising from the tape adhesive film (Scotch Magic) used as sample holder, and the peak shape analysis was performed by a least square fitting to the experimental data with an ensemble of generalized Lorentzian curves [8]. The oxygen content was analysed with a Oxygen leco system on the samples at the final milling stage. The oxygen concentration was between 3–4 at %.

3. Results

The compositions under investigation have been selected within or near the phase boundaries of the Ti_3Al(α_2-phase) and TiAl(γ-phase) intermetallic compounds. As a consequence the obtained results may be divided into two corresponding sections.

3.1. Ti_xAl_{100-x} (X = 80, 75 at %)

The X-ray diffraction patterns recorded with MoK_α radiation (Fig. 1) give the qualitative description of MA sequence for Ti_xAl_{1-x} (X = 80, 75 at %). In both cases, the mechanical alloying process induces an amorphous state after a certain milling time which strongly depends on the Al percentage. In fact, the $Ti_{75}Al_{25}$ composition (Fig. 1b) amorphized completely after 15 h of milling, whereas a prolonged processing up to 27 h has been necessary to promote the amorphization for $Ti_{80}Al_{20}$ (Fig. 1a) composition. The position of the maximum of the amorphous halo lies for the two compositions, within the experimental uncertainty, at the same angular position (2θ = 17.7°). The nearest neighbour distance of 0.28 nm, that can be estimated, in first approximation, by the Ehrenfest equation, is in agreement with previous measurements on the same composition [6] and corresponds to the weighted sum of atom radii of Al and Ti.

At X = 75, it is worth noticing that further MA leads to the crystallization of the amorphous phase into a new phase, with f.c.c. structure having a lattice parameter of a = 0.42 nm, as already observed in a sample of the same composition milled using a different ball mill [6].

From the high resolution patterns obtained after the early stage of MA(5 h of milling) with Co$K_{\alpha 1}$ radiation (Fig. 2a, b), it is clearly appreciable that the Ti(0 1 0) peak position shifts towards higher scattering angle. Furthermore, from the pattern of Fig. 1a, one can deduce that the highest shift is already reached at this point. Table I gives the peak positions as calculated by the fitting procedure. Since ball milling on pure Ti produces only a line broadening for this reflexion, the peak shift can be attributed to a shrinkage of lattice parameter due to the diffusion of Al into Ti promoting the formation of an hcp Ti(Al) solid solution. Clark *et al.* [9] measured the α-Ti(Al) solid solution lattice parameters as a function of Al content. According to their data, the amount of the dissolved Al can be estimated to be about 14–16 at %.

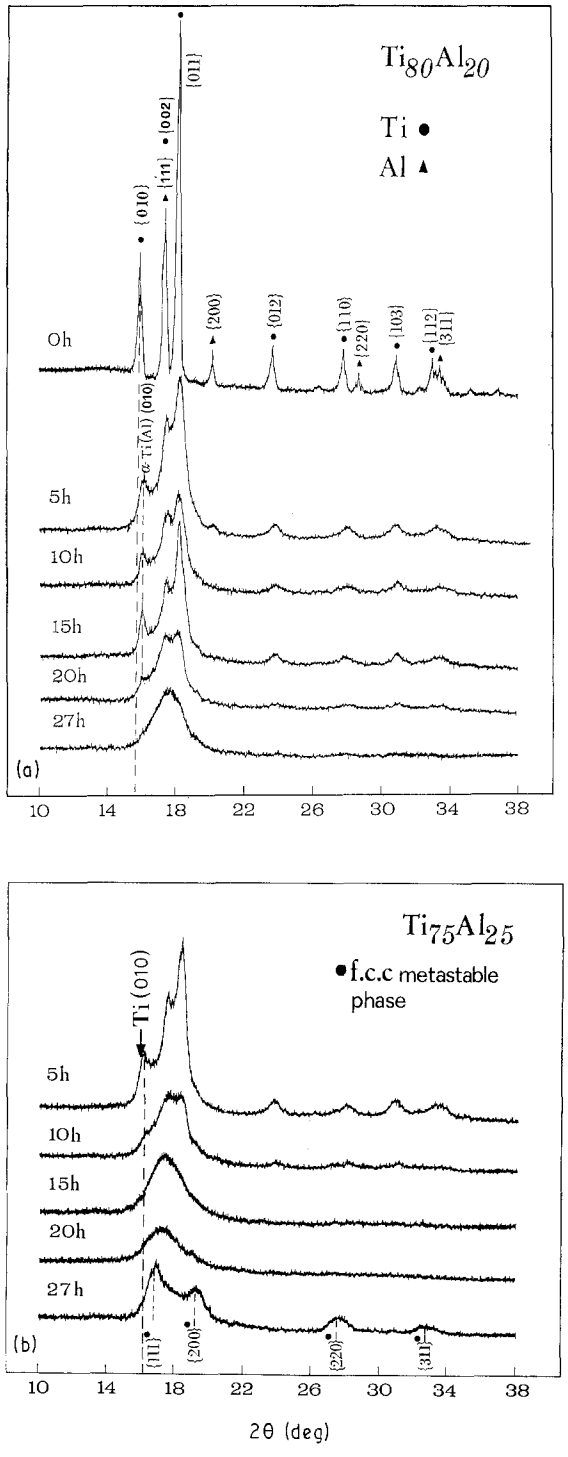

Figure 1 X-ray diffraction patterns at different milling times. (a) $Ti_{80}Al_{20}$, (b) $Ti_{75}Al_{25}$, (c) $Ti_{50}Al_{50}$ and (d) $Ti_{40}Al_{60}$ (used wavelength: MoK_α).

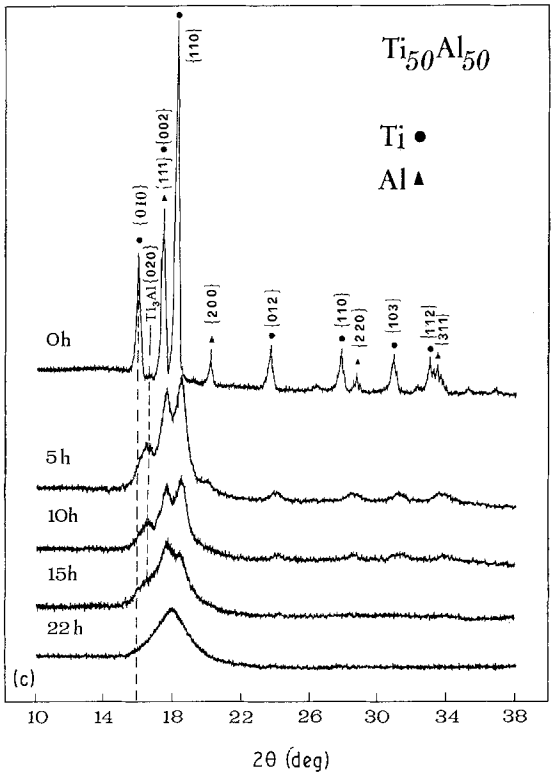

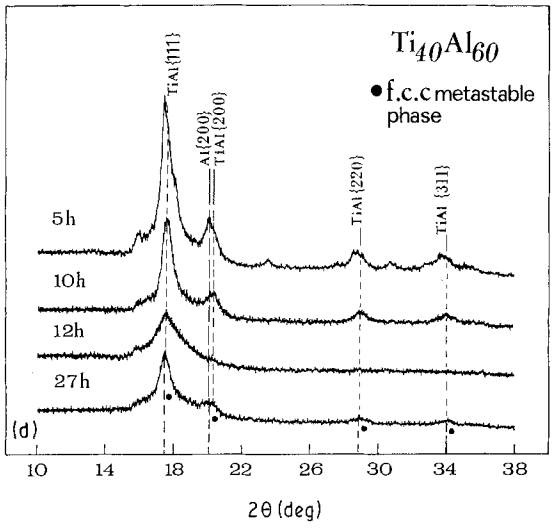

Figure 1 Continued.

3.2. Ti_xAl_{1-x} ($X = 50, 40$ at %)

For $X = 50$, apart from a longer time (22 h) required to amorphize the mixture (Fig. 1c) with respect to the $Ti_{75}Al_{25}$, a more accurate analysis (Fig. 2c) shows that after the first period of milling the peaks relative to Al almost completely disappear and that the shift of the Ti peaks is more accentuated. The angular positions of the most intense reflection might be ascribed after 5 h of milling to the fundamental reflections of the DO_{19} superstructure of the Ti_3Al intermetallic compound (ASTM N. 16-867). Since no superlattice reflections could be detected (see Fig. 3a), the whole pattern can be ascribed at the same time, either to a disordered form of the Ti_3Al structure, or to a supersaturated

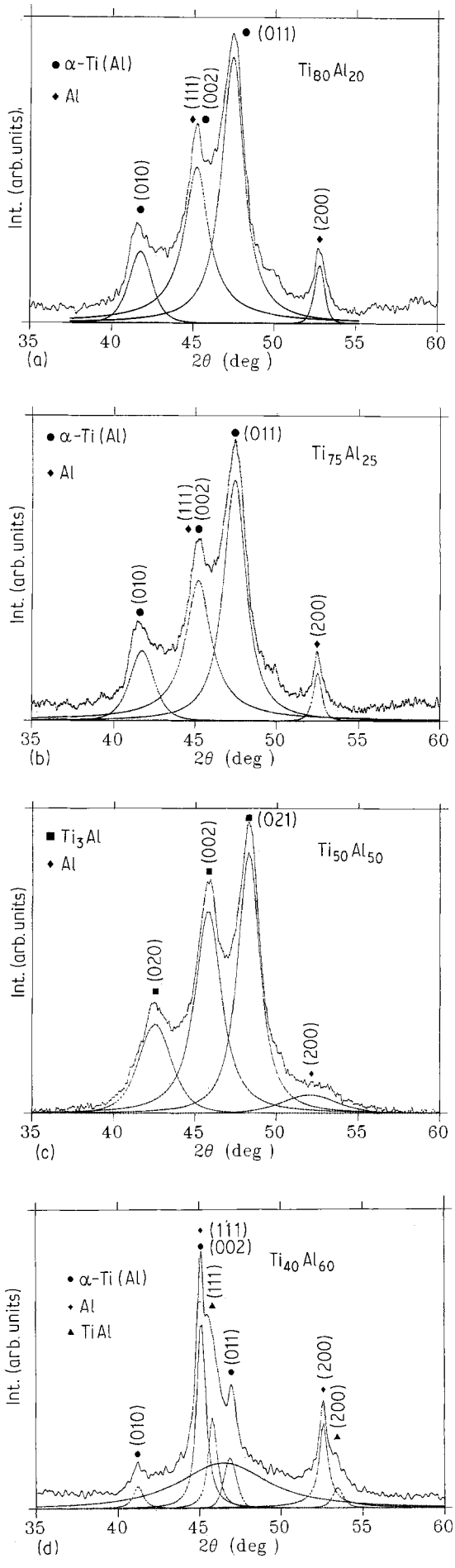

Figure 2 X-ray diffraction patterns of the early stage of alloying (5 h of milling). (a) $Ti_{50}Al_{20}$, (b) $Ti_{75}Al_{25}$, (c) $Ti_{50}Al_{50}$ and (d) $Ti_{40}Al_{60}$ (used wavelength: $CoK_{\alpha 1}$). The Lorentzian peak components after the fitting procedure are also shown. The *d*-values are reported in Table I.

TABLE I Lattice spacing of the main reflections of the h.c.p. Ti(Al) solid solution, pure Al, Ti_3Al and TiAl intermetallic compounds, as determined by the fitting procedure. *Note*: Ti(0 1 0), $d = 0.2557$ nm

Alloy	$Ti_{80}Al_{20}$	$Ti_{75}Al_{25}$	$Ti_{50}Al_{50}$	$Ti_{40}Al_{60}$
1	0.2530 nm αTi(Al)(0 1 0) Al 16 at %	0.2532 nm αTi(Al)(0 1 0) Al 15 at %	0.24718 nm Ti_3Al(0 2 0)	0.2543 nm αTi(Al)(0 1 0) Al 7 at %
2	0.2332 nm αTi(Al)(0 0 2) + Al(1 1 1)	0.2328 nm αTi(Al)(0 0 2) + Al(1 1 1)	0.2298 nm Ti_3Al(0 0 2)	0.2331 nm αTi(Al)(0 1 0) + Al(1 1 1)
3				0.2294 nm TiAl(1 1 1)
4	0.222 nm αTi(Al)(0 1 1)	0.2225 nm αTi(Al)(0 1 1)	0.2189 nm Ti_3Al(0 2 1)	0.2244 nm αTi(Al)(0 1 1)
5	0.203 nm Al(2 0 0)	0.2028 nm Al(2 0 0)	0.203 nm Al(2 0 0) very weak	0.2025 nm Al(2 0 0)
6				0.1988 TiAl(2 0 0)

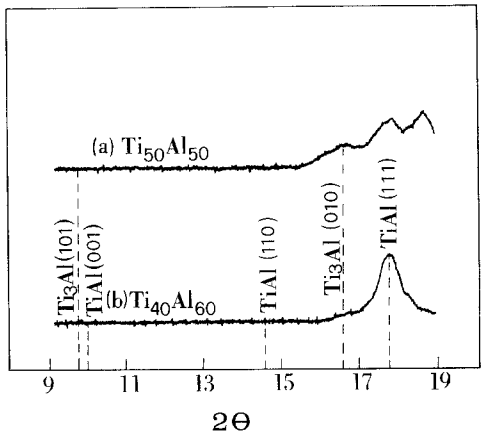

Figure 3 Low angle part of MoK_α diffraction patterns of the (a) $Ti_{50}Al_{50}$, and (b) $Ti_{40}Al_{60}$ compositions after 10 h of milling. The angular positions of the superstructure reflections are indicated.

α(Ti) solid solution with an Al content $\geqslant 30\%$, because both phases present the same unit cell.

As it concerns the $Ti_{40}Al_{60}$ composition, a distinct alloying path is clearly recognizable. The diffraction pattern after 5 h of MA (Fig. 2d) points out the nucleation onset of the TiAl intermetallic compound (ASTM N. 5-678), which is completed after additional 5 h of MA (Fig. 1d). The only occurrence of reflections, whose indices are all odd or all even, evidences that the TiAl intermetallic holds an Al–f.c.c. structure, without forming the L1o layered superlattice (Fig. 3b). The peak shift of the Ti(0 1 0) is less pronounced, corresponding to an Al content of 7%, indicating a preferential path towards the intermetallic compound formation. An amorphous component, whose maximum is located at the same angular position as for the other compositions, is also detectable after the early stage of alloying. In the present case, the highest degree of amorphization is achieved after 12 h (see Fig. 1d), however the irregular shape of the broad maximum indicates that besides an amorphous component additional contributions of a presumably crystalline phase are still superimposed. Upon further milling some crystalline reflections became more appreciable and, after 27 h of MA, the powder pattern is the sum of an amorphous contribution and of a crystalline phase whose structure can be tentatively indexed as a f.c.c. one with a lattice parameter $a \approx 0.41 \pm 0.05$ nm.

4. Discussion

4.1. Ti_xAl_{1-x} ($X = 80,75$ at %)

Recalling the thermodynamic model developed by Cocco *et al.* [6], the main feature of the Ti–Al system, assuming a kinetic inhibition of the intermetallics compound, can be summarized as follows: the amorphization window opens, at room temperature, to an Al concentration of about 20 at %, and all the compositions investigated here are, in principle, able to access the amorphous state. In more detail, the free energy curves [6], calculated at 0 °K (Fig. 4), evidence

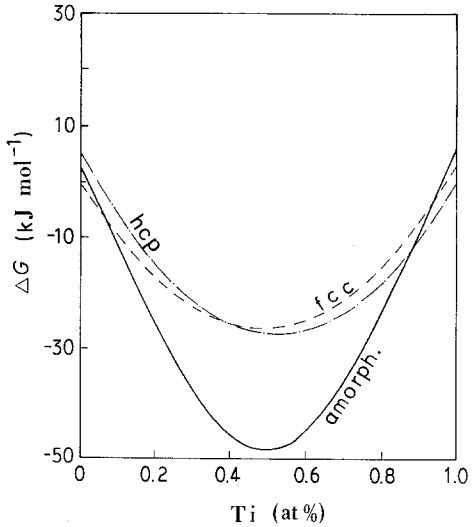

Figure 4 Free-enthalpy curve for Al–Ti at 0°K [6]. The amorphous phase is computed according to the Miedema model. The hcp and f.c.c. solid solutions are calculated with an equation taken from [20].

an Al amount of about 15%. Their free energy difference, hence the stability of the amorphous phase, increases sharply with the Al content reaching its maximum at the equiatomic composition.

Our experimental findings confirm that MA induces, as a first step, the solution of some amounts of Al into hcp Ti. The hexagonal α-Ti phase is supersaturated by Al atoms, up to a certain value beyond which the system collapses into the amorphous state. The measured Al concentration is about 14–16 at % in very good agreement with the theoretical prediction. It is worth noting that the critical Al content for the solid solution to transform into the amorphous phase is equal for both the starting mixtures, which confirms that this value, as long as the formation of intermetallic compound is kinetically suppressed, is independent from the starting composition. The pattern sequences shown in Fig. 1a, b suggest that the mechanism proposed for the amorphization of Zr–Al [4], based on the elastic instability of the solid solution, holds also in the present case. In fact the angular position of the Ti (0 1 0) reflection remains unaffected by further milling beyond 5 h, and a decrease of its integrated intensity corresponds to the apparence of an amorphous halo until the complete amorphization of the powder. The Al concentration of 14–16 at % can be, therefore, considered as an upper boundary for the solid solution, where the free energy of the crystalline and amorphous phases become equal.

Considering the time scale of the reaction one notes that the complete amorphization is achieved, for the $Ti_{75}Al_{25}$ composition, in a time markedly shorter than the one required for $Ti_{80}Al_{20}$. Because both starting powders were milled under identical conditions, this effect cannot only be ascribed to the uncertainty of the preparative method, but clearly states the strong influence of the Al content on the reaction path.

As has already been mentioned, the $Ti_{75}Al_{25}$ composition crystallizes in a f.c.c. structure after 27 h of MA, in a quite similar way to $Zr_{50}Al_{50}$ [4]. A possible explanation of this behaviour will be discussed in more detail.

4.2. Ti_xAl_{1-x} (50, 40 at %)

The behaviour of the $Ti_{50}Al_{50}$ composition seems to contradict the results obtained for the two Ti-rich mixtures. In fact, as previously said, the Al content after 5 h of milling should amount to about 30%, a value which is far beyond the solubility limit measured for the Ti of 75 and 80 at % compositions. This discrepancy can be solved by deciding for the nucleation of the disordered Ti_3Al rather than for a supersaturated solid solution.

The high negative heat of mixing combined with the local temperature rise during ball impact might be, in fact, sufficient to promote the nucleation of the intermetallic compound, but, at the same time, not high enough to climb over the energy barrier associated with the hcp A3 → DO_{19} (A_3B type) first type order transition. Ti_3Al, presupposes an elevated diffusion of both the constituent elements. The low mobility of both atom sorts, at the temperature at which this SSR takes place, may explain the suppression of the ordering transition.

The nucleation of an intermetallic compound alters substantially the evolution of the alloying process, since it lowers the energy of the system.

As a consequence, the transition to the glassy state, which remains favoured by MA, as demonstrated by the experimental results, is attained mainly through a destabilization of the crystalline structure. The step through the intermetallic phase, instead of a straightforward reaction to the amorphous phase, may also explain the different milling time required to completely amorphize the $Ti_{50}Al_{50}$ composition.

Owing to the composition of the starting powder, the assumed disordered Ti_3Al metastable phase is driven, upon prolonged milling, far from its chemical equilibrium, as can be deduced by the homogeneity range of the ordered Ti_3Al intermetallic (22 to 39 Al at %) [10], causing again the crystalline phase to become unstable and to transform into the amorphous phase, under the assumption that the nucleation of a more stable intermetallic phase such as TiAl is suppressed.

The suppression of the nucleation of the TiAl intermetallic compound is clear in the diffraction pattern (Fig. 2c), although the starting powder has been selected close to the stoichiometry of this equilibrium phase.

Assuming that the fast diffusion of Al avoids possible local Al enrichments, one can reasonably consider that the average concentration of Al diffused into the Ti matrix remains during milling below the value of the starting mixture. Moreover observing that the compositional range of existence of the TiAl intermetallic compound admits a minimum Al content of about 48–49 at %, it is plausible to suppose that during the MA process the prerequisites for the formation of the TiAl intermetallic, as it concerns the chemical composition, the negative heat of mixing and the energy imparted to the system are not fulfilled. The above assumption is indirectly confirmed by the reaction path of the $Ti_{40}Al_{60}$ composition.

The diffraction pattern (Fig. 2d) clearly indicates the formation of the A1–f.c.c. TiAl intermetallic already after first sampling time (5 h). The involved mechanism of the intermetallic compound formation appears to be quite similar to the one observed for the $Ti_{50}Al_{50}$ composition. However, the higher Al initial contents allows, in this case, the system to reach, during ball milling, the appropriate chemical composition for nucleating the TiAl phase. The total absence of the (0 0 1) and (1 1 0) lines (Fig. 3b), which are characteristic of the L1o–TiAl superlattice, confirms even in this case the lack of long range order. It is worth noticing that the critical temperature of the order/disorder transition is near the melting point of TiAl phase ($\approx 1450\,^{\circ}C$) [10], and at room temperature the TiAl phase is always present in its ordered state. The low

temperature SSR induced by MA discloses the existence of disordered phases [11], which are not attainable with conventional preparation techniques.

According to the analysis of Fig. 2d, it also appears that the Ti(0 1 0) peak shift is less accentuated, corresponding to an Al concentration in the h.c.p.-solid solution of about 7 at %, and that an amorphous component can be singled out from the total scattering curve. The simultaneous occurrence of different phases together with the low Al content of the hcp solid solution indicates that the required Al concentration to form an amorphous or an intermetallic phase is reached promptly during ball impact in the given milling condition.

The contemporaneous formations of an amorphous component and an intermetallic compound as well indicate that the two reaction paths are competing with each other [12]. The nearly equal heat of formation for the amorphous phase ($\approx -45\,\mathrm{kJ\,mol^{-1}}$, see Fig. 4) and the equilibrium intermetallic compound, experimentally measured at room temperature for an Al content of 60 at % ($-40 \pm 2\,\mathrm{kJ\,mol^{-1}}$) [13], may explain the simultaneous nucleation of these phases and the consequent partial amorphization of the powder.

The previous considerations about off-stoichiometric composition do not hold for the present case, because of the wide range of homogeneity (48 ~ 66 at % Al) of the TiAl intermetallic phase. Furthermore, since the TiAl intermetallic phase already appears in its disordered form, an increase of the stored internal energy by a loss of long range order in the crystalline structure, as, for instance, observed in MA of CsCl-type [14] or Ni_3Al [15] intermetallic compounds, can be presently neglected. The kinetic constrains together with the negligible difference in the heat of formation may incline the reaction path towards the amorphous state, meanwhile the MA does not raise the free energy of the TiAl intermetallic phase to the necessary amount, of about $10 \sim 15\,\mathrm{kJ\,mol^{-1}}$ [16], which allows stabilization of the amorphous state.

4.3. Metastable f.c.c. phase

The appearance, for $Ti_{75}Al_{25}$ and $Ti_{40}Al_{60}$ compositions under prolonged milling (27 h), of reflection peaks which can be ascribed to an f.c.c. crystalline structure (see Fig. 1b and d) suggests that MA may promote the formation of a metastable solid solution of Ti–Al over a wide range of compositions. Taking into account that in the nucleation by MA stable ordered phases are inhibited, it is plausible to suppose that the atoms of Ti and Al are randomly distributed within the supposed f.c.c. lattice. From the data reported in the literature it can be seen that the stable TiAl intermetallic phase has a face centered tetragonal structure ($a = 0.3984$, $c = 0.4065$, $c/a = 1.02$, Al 52%) very close to an f.c.c. one, whose c/a ratio slightly changes with the Al content. The existence of this phase could suggest a transformation induced by milling towards this kind of geometry, and, at the mean time, that the structure of the metastable phase might

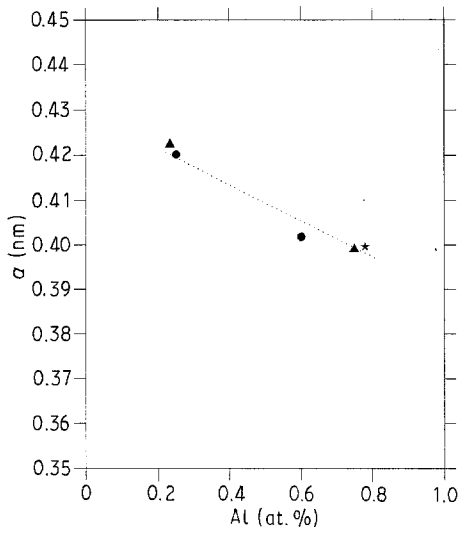

Figure 5 Lattice parameter of the f.c.c. metastable phase plotted as a function of Al content (▲) for [6], (*) for [17] and (●) for present work. The points are connected with an interpolating line for clarity.

be considered only approximately as an f.c.c. one. In any case, the different amounts of the smaller Al atoms forming the solid solution would alter the volume of the unit cell and, as a consequence, the value of the lattice constant as determined by the f.c.c. indexing of the reflections.

In Fig. 5, the values of the lattice constant are plotted together with the ones measured by Cocco *et al.* [6] as a function of the Al content. On the same plot the lattice parameter of a metastable f.c.c. Al_3Ti phase formed by ion beam mixing and thermal annealing in codeposited AlTi multilayer [17] is also reported. The dependence of the a lattice parameter, hence of the volume of the unit cell is linear with the Al concentration, and the shrinkage of the volume agrees with different atomic radii of Ti and Al. The evidence that SSR induced by ball milling does not always end in an amorphous state, is nowadays well documented in the literature [4, 18, 19]. The almost linear dependence of the lattice parameter is indicating the occurrence of a polymorphous nucleation of the simple f.c.c. structured metastable phase. In the present investigation we do not obtain the crystallization of $Ti_{50}Al_{50}$ composition, which lies between the proposed range of formability of the fcc metastable phase. We believe that this effect, as well as the very weak intensities observed in the case of the $Ti_{40}Al_{60}$ composition, is probably due to insufficient applied milling times. Further work is in progress to characterize in more detail the compositional and temperature range of this metastable phase.

5. Conclusion

(a) Ti_xAl_{1-x} alloys have been successfully amorphized by MA in the composition range $50\% \leqslant X \leqslant 80\%$. On the Ti rich side, the value experimentally determined exactly hits the theoretical prediction, whereas on the Al rich side the limiting

factor is represented in the present milling conditions by the nucleation of TiAl intermetallic compound.

(b) Depending on the starting composition the SSR induced by MA follows two different paths: the Ti rich mixtures form firstly a hcp solid solution, which, in turn, collapses into the amorphous state. Ball milling the Al rich composition ($Ti_{50}Al_{50}$ and $Ti_{40}Al_{60}$) leads to formation of intermetallic compounds, as an intermediate state of the reaction path. Due to the low temperature at which the SSR takes place the Ti_3Al and TiAl phases present a disordered structure characterized by the absence of superlattice reflections.

(c) Prolonged milling causes the polymorphous nucleation of a f.c.c. metastable phase for the $Ti_{75}Al_{25}$ and $Ti_{40}Al_{60}$.

References

1. Y. W. KIM, *J. O. M*, **41** (July 1989) 24.
2. E. ARTZ and L. SCHULTZ, "New Materials by Mechanical Alloying Techniques" (DGM, Oberursel, 1989).
3. S. MARTELLI, G. MAZZONE, S. SCAGLIONE and M. VITTORI ANTISARI, *J. Less Common Metals* **145** (1988) 261.
4. H. J. FETCH, G. HAN, Z. FU and W. L. JOHNSON, *J. Appl. Phys.* **67** (4) (1990) 1744.
5. L. SCHULTZ, *Mat. Sci. Eng.* **97** (1988) 15.
6. G. COCCO, I. SOLETTA, L. BATTEZZATI, M. BARICCO and S. ENZO *Phil. Mag. B* **61** (1990) 473.
7. R. SUNDARESAN, A. G. JACKSON, S. KRISHNAMURTHY and F. H. FROHES, *Mat. Sci. Eng.* **97** (1988) 115.
8. D. W. MARQUART, *J. Soc. Ind. Appl. Math.* **91** (1963) 431.
9. W. B. PEARSON, "Handbook of lattice spacings and structures of metals" (Pergamon Press, Oxford, 1967).
10. T. B. MASSALSKY, "Binary Phase Diagrams" (A.S.M., 1986).
11. S. MARTELLI, G. MAZZONE, A. MONTONE, F. PADELLA and M. VITTORI "EUROMAT '89" (Aachen, Oberursel, 1989).
12. M. MAGINI, F. PADELLA, G. ENNAS, F. POMPA and M. VITTORI, *J. Non Cryst. Solids* **110** (1989) 69.
13. (a) O. KUBASCHEWSKY and W. A. DENCH, *Acta Met.* **3** (1955) 339; (b) O. KUBASCHEWSKY and G. HEYMER, *Trans. Faraday Soc.* **56** (1960) 473.
14. E. HELLSTERN, H. J. FECHT, A. FU and W. L. JOHNSON, *J. Mat. Res.* **4** (1989) 1292.
15. J. S. C. JAN and G. C. KOCH, *J. Mat. Res.* **5** (1990) 498.
16. A. BLATTER and M. VON ALLMEN, *Mat. Sci. Eng.* **97** (1988) 93.
17. Q. Z. HONG, D. A. LILIENFELD and J. W. MAYER, *J. Appl. Phys.* **64**(a) (1989) 4478.
18. F. PETZOLDT, B. SCHOLZ and H. D. KUNZE, "New Materials by Mechanical Alloying Techniques", edited by E. Artz and L. Schultz (DUM, Oberursel, FRG, 1989).
19. A. BLATTER and M. VON ALLMEN, *Phys. Rev. Lett.* **54** (1985) 2103.
20. J. L. MURRAY, *Metall. Trans.* **19A** (1988) 243.

Received 1 October 1990
and accepted 31 January 1991